Tropical Journal of Natural Product Research

Available online at https://www.tjnpr.org

Original Research Article

Biopolymer Nanoencapsulation of *Andrographis paniculata* (Burm. f.) Nees and Carboxymethyl Chitosan for Dengue Therapy

Browi Nugroho[1], Sari E. Cahyaningrum[1]*, Pirim Setiarso[1], Andika P. Wardana[1], Teguh H. Sucipto[2]

[1]*Department of Chemistry, Faculty of Mathematics and Natural Sciences, Universitas Negeri Surabaya. Jl. Ketintang, Gayungan, Surabaya 60231, East Java, Indonesia.*
[2]*Dengue Study Group, Institute of Tropical Disease, Universitas Airlangga. Jl. Dr. Ir. H. Soekarno, Mulyorejo, Surabaya 60115, East Java, Indonesia.*

ARTICLE INFO

ABSTRACT

Dengue fever is a global health problem, with millions of cases reported each year. The lack of available therapeutic agents has stimulated the search for new treatments. This study aimed to synthesize, and characterize biopolymer-based nanoencapsules using *Andrographis paniculata* and carboxymethyl chitosan (CMC), and evaluate their activity against dengue virus. *A. paniculata* nanocapsules (AP-NPs) were formulated by ultrasonication of *A. paniculata* extract with carboxymethyl chitosan. AP-NPs were characterized by particle size analysis, Fourier Transform Infrared (FTIR) analysis, and stability under various conditions of pH, temperature, and electrolyte (NaCl). The antiviral activity against dengue virus (DENV-2), and cytotoxic activity against Vero cell line were evaluated according to standard procedures. AP-NPs was successfully synthesized with particle size of 305.5 ± 30.12 nm, and a polydispersity index (PDI) of 0.3319 ± 0.01. AP-NPs had improved stability and better controlled release of bioactive components than *A. paniculata* extract. AP-NPs had a loading amount of $27.18 \pm 2.51\%$, and a loading efficiency of $54.36 \pm 5.02\%$. AP-NPs exhibited enhanced antiviral activity and bioavailability compared to the pure *A. paniculata* extract, although with increased cytotoxicity. The CC_{50} of AP-NPs was 734.56 µg/mL, which was significantly lower than that of the extract (1522.95 µg/mL), while the EC_{50} for AP-NPs was 68.12 µg/mL, compared to 9.87 µg/mL for the extract. Despite the higher toxicity, AP-NPs offer promising potential as a therapeutic candidate for dengue fever, particularly due to their ability to improve bioavailability and provide sustained antiviral effects.

Keywords: Andrographis paniculata, Carboxymethyl chitosan, Antiviral, Dengue, Controlled release.

Introduction

Since the beginning of 2024, more than 14 million dengue cases and over 10.000 fatalities have been documented worldwide, with the majority occurring in the region covered by the World Health Organization's Pan American Health Organization. This region recorded over 12 million cases, 53% lab-confirmed, and more than 7.000 deaths. Brazil recorded the highest number of cases (over 9.8 million), followed by Argentina, Mexico, Colombia, and Paraguay as of November 2024.[1] Dengue virus is a viral RNA in the genus Flavivirus, family Flaviviridae which is transmitted through mosquito bites, leading to Dengue Hemorrhagic Fever (DHF). The Dengue virus is classified into four distinct serotypes (DENV1-4).[2] with dengue-2 virus (DENV-2) contributing seriously to death from dengue fever.[3] Therapeutic agents under investigation fall into two categories: pathogen-neutralizing antibodies and antiviral peptides, both designed to disrupt viral entry into host cells.[4] However, no therapeutic agents for dengue fever are presently approved for clinical application.

*Corresponding author. E mail: saricahyaningrum@unesa.ac.id
Tel: +62-812-3290-484

Medicinal plant species generally contain secondary metabolites, such as steroids, phenolics, tannins, alkaloids, anthocyanins, flavonoids, and saponins.[6] *Andrographis paniculata* (*A. paniculata*) has been traditionally utilized in several countries for its diverse biological activities, including antioxidant, antidiabetic, antidiarrheal, anticancer, anti-inflammatory, antiviral, antifungal, antimalarial, cardiovascular, cytotoxic, hepatoprotective, and antihypertensive properties.[7] *A. paniculata* thrives in lowland regions up to an altitude of 700 meters, preferring temperatures of 25-32°C, moderate humidity, and adequate light intensity, with an optimal soil pH of 5.5-6.5. Its leaves are rich in diterpene lactones and glycosides, such as andrographolide, deoxyandrographolide, 11,12-didehydro-14-oxoandrographolide, neoandrographolide, as well as flavonoids.[8] As an antidengue agent, *A. paniculata* exhibits 75% inhibition of dengue virus with 55%–97% cell viability in DENV-1–4 infected cells. The active compounds detected include; terpenoids (andrographolides) and flavonoids (luteolin, quercetin, kaempferol, and wogonin).[9–11] The effectiveness of quercetin as an antiviral agent against DENV-2 has been demonstrated, and the compound showed high effectivity with CC_{50}, IC_{50}, and SI values of 217.113 µg/mL, 18.406 µg/mL, and 11.797, respectively, indicating its potential as an antiviral agent against DENV-2.[12]

About 90% of clinical drug development fails due to low effectiveness and lack of specificity. During drug development process, the distribution of the drugs to various body tissues, which is an important parameter that contributes to drug effectiveness and safety is often ignored. This can lead to inappropriate drug candidate selection and difficulties in determining effective doses without causing harmful side effects.[13] Some active compounds are damaged or degraded by extreme conditions, such as a very acidic pH within the human

168

Trop J Nat Prod Res, January 2025; 9(1): 168 - 175   **ISSN 2616-0684 (Print)**
ISSN 2616-0692 (Electronic)

digestive tract, and this results in low concentration of active compounds that reach systemic circulation.[14,15]

Natural polymers are more commonly used as coating agents because they are non-toxic, bioavailable, biocompatible and biodegradable. The types of natural polymers that are often used as coatings for encapsulation techniques are chitosan, casein, starch, whey protein, albumin, and alginate.[16–18] Chitosan is a biopolymer that is biocompatible, biodegradable, with an excellent adsorption properties, good release profile of active compounds, good stability, low toxicity, and simple method of preparation. Chitosan has limited application in drug delivery systems because it is insoluble at neutral pH, only soluble in acidic environments. As a result, the ability of chitosan to dissolve in the gastrointestinal tract is limited to the duodenum.[19,20] Meanwhile, 90% of drug absorption occurs in the small intestine, especially the jejenum where most of the digestion and chemical absorption occur making permeability in this part crucial for drug effectiveness.[21,22] One of the promising derivatives is carboxymethyl chitosan. Carboxymethyl chitosan (CMC) is a chitosan derivative that has a wide range of applications in drug delivery system, and biomedical sciences, including cosmetic, food preservation, biosensors, and emulsion stabilization. In addition, the pKa (2.0 - 4.0) of CMC provides great potential to overcome chitosan solubility problem, and extend the drug absorption site beyond the duodenum.[23]

Nanoencapsulation, a nanotechnology application that enhances the protection and bioavailability of bioactive compounds by increasing surface area and stability at the nanoscale,[24] was applied in the current study. The study therefore aimed to synthesize and characterize *A. paniculata* encapsulated with carboxymethyl chitosan, and investigate its antiviral potential against the dengue virus *in vitro*.

Materials and Methods

Materials
A. paniculata, methanol, distilled water, carboxymethyl chitosan, HCl (Merck), NaCl (Merck), KCl (Merck), $Na_2HPO_4.2H_2O$ (Merck), $NaH_2PO_4.H_2O$ (Merck), quercetin (Sigma-Aldrich), vero cell (ATCC® CCL-81™), fetal bovine serum (FBS), phosphate buffered saline (PBS), Dengue Virus Serotype 2 (NCBI No. KT012513, Dengue Study Group, Institute of Tropical Disease, Universitas Airlangga), viral ToxGlo reagent (Promega), CellTiter-Glo® Luminescent Cell Viability Assay kit (Promega), Minimum Essential Medium Eagle (MEM), and 3-(4,5)-dimethylthiazole-2-yl)-2,5-diphenyltetrazolium bromide (MTT), were utilized in the study.

Extraction of A. paniculata
Dried powdered *A. paniculata* leaves (1 kg) was extracted by maceration in methanol at room temperature for 24 hours. The extraction process was done three times. The combined methanol extract was filtered using vacuum filtration, and then concentrated *in vacuo* using a rotary evaporator (BUCHI R-300, USA).

Nanoencapsulation of A. paniculata
Nanoencapsulation of *A. paniculata* was carried out by ultrasonication method. *A. paniculata* extract was dissolved in methanol and mixed with carboxymethyl chitosan. The mixture was then sonicated in a sonicator (Elmasonic S 30, Germany) for 30 minutes without heating until a homogeneous nanocapsule solution was obtained.[24]

Characterization of A. paniculata nanocapsule (AP-NPs)
The physicotechnical characteristics of *A. paniculata* (AP) and AP-NPs were assessed by measuring the polydispersity index (PDI) and particle size using a Particle Size Analyzer (Zetasizer Nano ZS, Malvern, UK). The functional groups of AP and AP-NPs were identified using a Fourier Transform Infrared (FTIR) spectrophotometer (Perkin Elmer FTIR Spectrum Two, UK).

Assessment of stability of AP-NPs
The stability of *A. paniculata* and AP-NPs in preserving bioactive compounds was evaluated using several parameters, including temperatures (30 - 100°C), pH (2 - 10), and NaCl concentrations (0 - 0.3 M). Additionally, the UV-Vis absorption spectrum (Shimadzu UV-1800, Japan) was measured for each parameter, and nanoparticle

turbidity was assessed using a turbidimeter (Milwaukee Mi415, USA).[25]

Assessment of loading and release of AP-NPs
One of the key physicotechnical parameters is drug loading, which is defined as the ratio of the mass of the drug to the nanoparticles loaded by the drug.[26] The drug loading process of AP-NPs was carried out by dialysis using a membrane with a size of 14 kDa (Dialysis Tubing 12-14 kDa Sigma-Aldrich, Germany). The amount of loading (LA) and loading efficiency (LE) for each bioactive component were determined using Equations 1 and 2, respectively. The release of bioactive compounds from AP-NPs was assessed using Equation 3. Loading and discharge measurements were performed by measuring the absorbance using a UV-Vis spectrophotometer.[26]

$$\% \, LA = \frac{Mass \; of \; samples \; on \; AP-NPs}{Mass \; of \; samples \; in \; feed} x100\% \qquad (1)$$

$$\% \, LE = \frac{Mass \; of \; samples \; on \; AP-NPs}{Mass \; of \; AP-NPs} x100\% \qquad (2)$$

$$Ct' = Ct + \frac{v}{V}\sum_{0}^{i-t} Ct \qquad (3)$$

Where;
Ct' = Correction of concentration at time t
Ct = Measurement of concentration at time t
V = Total buffer volume used
v = Aliquot Volume

Determination of antidengue activity
The antiviral activity against DENV-2 was conducted following the method of Sucipto *et al*. (2019)[27] with minor modifications. Vero cell lines were used for the assay. Confluent monolayers of Vero cells (5×10^4 cells/mL) were seeded in a 96-well plate and incubated at 37°C for 24 hours in a 5% CO_2 atmosphere. After removing the medium, 50 μL of MEM containing 10% FBS was added, followed by 25 μL of samples (*A. paniculata* and AP-NPs) at concentrations of 1, 10, and 100 μg/mL, and 25 μL of DENV-2 stock at 2×10^3 FFU/mL. This procedure was repeated three times. The samples were then incubated for 48 hours at 37°C with 5% CO_2. Following incubation, 100 μL of Viral ToxGlo reagent was added and the samples were incubated again at 37°C with 5% CO_2. The luminescence data obtained was then calculated as percentage of CPE (cytopathic effect) using the formula:

$$\% \, CPE = \frac{a-b}{c-b} x100\% \qquad (4)$$

Where; a = luminescene treatment; b = luminescence control medium; c = luminescence (DENV-2 control + cell control). From the % CPE data, a linear regression graph of concentration vs % CPE was made, y = ax + b, where x = concentration and y = % CPE to determine EC_{50}.

Cytotoxicity test
The cytotoxicity test on Vero cell lines was performed using the MTT method.[27] Confluent monolayers of Vero cells (5×10^4 cells/mL) were seeded in 96-well plates and incubated for 24 hours at 37°C in a 5% CO_2 atmosphere. After removing the medium, the cells were washed three times with 1× PBS. Then, 100 μL of MEM with 10% FBS was added, followed by 100 μL of the samples (*A. paniculata* and AP-NPs) at concentrations of 100, 250, and 500 μg/mL, and incubated for another 24 hours at 37°C with 5% CO_2. This procedure was repeated three times. After incubation, the culture medium containing the samples was discarded, the cells were washed with 100 μL of PBS, and 10 μL of MTT reagent was added. The cells were then incubated for another 4 hours, followed by a PBS wash. The absorbance was read at 595 nm using a microplate reader. The percentage of live cells was calculated using the formula:

$$\% \, live \; cell = \frac{a-b}{c-b} x100$$

Where; a = absorbance of media with treatment; b = absorbance of media without treatment (media control); c = absorbance of cell without treatment (cell control).
A linear graph of concentration vs percentage of live cells was prepared to determine CC_{50}

© 2024 the authors. This work is licensed under the Creative Commons Attribution 4.0 International License

Results and Discussion

Extraction yield of A. paniculata
The extraction process of *A. paniculata* produced a thick extract (90 g) from 1 kg of the dried powdered sample, resulting in an extract yield of 9%.

Quercetin standard curve
Standardization of *A. paniculata* was carried out against the quercetin standard. The linear regression equation for the quercetin standard curve was $y = 0.0831x - 0.0057$ with $R^2 = 0.9963$ (Figure 1).

Table 1: Physiochemical properties of *A. Paniculata* nanocapsule

Parameter	Value
Particle Size (nm)	305.5 ± 30.12
PDI	0.3319 ± 0.01

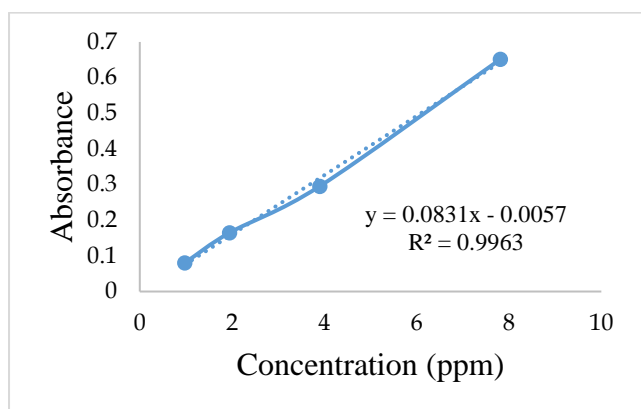Values are Mean $\pm$ Standard Deviation (SD). PDI = Polydispersity index

Figure 1: Quercetin standard curve

Physicotechnical characteristics of A. paniculate nanocapsule
Nanoencapsulation produces nanocapsules, which are vesicular systems of bioactive compounds surrounded by polymer membranes with a maximum particle size of 500 nm.[28] *A. paniculata* nanocapsules (AP-NPs) formulated with the biopolymer carboxymethyl chitosan were characterized by their particle size and polydispersity index (PDI) as shown in Table 1.
Particle size are measured to ensure that the resulting nanocapsules are within the nanoparticle size range. In addition, polydispersity index (PDI) is used to describe the degree of non-uniformity of particle size distribution otherwise known as the heterogeneity index.[29] Table 1 shows that the particle size of AP-NPs is 305.5 ± 30.12 nm, which indicates that the nanoencapsulation process of AP-NPs successfully met the criteria of nanoparticles. In addition, the PDI AP-NPs value of 0.3319 ± 0.01 indicates that the particle size is relatively homogeneously distributed. Generally, a PDI ≤ 0.05 indicates a very uniform size distribution. In contrast, PDI ≥ 0.7 indicates a more varied and less uniform particle size distribution.[30] In this study, the nanoencapsulation process used an ultrasonication technique. Ultrasonication is able to control the particle size through the phenomenon of acoustic cavitation which helps to break down the particle aggregate into smaller individual particles.[30]
FTIR characterization was done to ensure that the AP-NPs have the typical functional groups of *A. paniculata* and carboxymethyl chitosan. The FTIR spectrum of AP-NPs showed a shift in the absorption band in the 3323 cm⁻¹ region indicating an overlap of the -OH and -NH groups, but with a slight shift compared to pure CMC, which may indicate an interaction between the quercetin of *A. paniculata* and CMC (Figure 2).
In AP-NPs FTIR spectrum, an absorption band at 2924 cm⁻¹ is a persistent C-H stretch, indicating that the aliphatic component is

maintained. Peaks at 1583 and 1405 cm⁻¹ indicate C=O stretching of the amide, with slight shifts that may indicate an interaction between the C=O group on the CMC and the active component of *A. paniculate*. The peak at 1019 cm⁻¹ indicates an interaction between the C-O-C group in the CMC and the components of *A. paniculata*.

Stability of A. paniculate nanocapsule
The stability of herbal extract nanoencapsulation in this case AP-NPs under various environmental conditions, such as temperature, pH, and salt concentration, is an important parameter for assessing the durability and effectiveness of the nanoencapsulation system. The following are the results and explanations of the effects of each of these conditions.
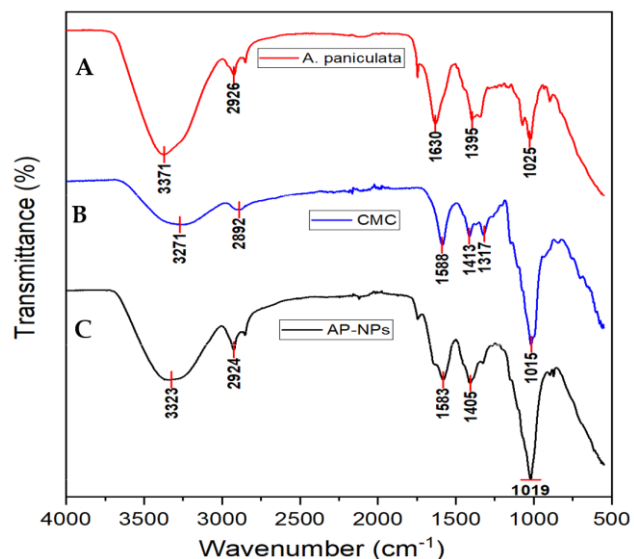

Figure 2: FTIR spectra of **(A)** *A. paniculata*, **(B)** CMC and **(C)** AP-NPs

The stability of AP-NPs and *A. paniculata* was carried out at different pH ranging from 2 to10. The stability level was assessed by taking spectral readings using UV-Vis spectrophotometer, and turbidity using a turbidimeter. The effect of pH on the UV-Vis spectrum is shown in Figure 3. The UV-Vis spectrum of *A. paniculata* (Figure 3A) showed significant changes in various pH conditions. At first, the solution had a pH of 5. When the pH was lowered to 2-4, there was a significant decrease in absorbance intensity, indicating a hypochromic shift. This indicates a degradation or strong interaction with the acidic environment, so the ability of the molecules to absorb light decreases. In contrast, at pH 6-10, the absorbance intensity increased, with a more significant hyperchromic shift at pH 7-10. This increase suggest a change in the electronic environment of the active molecule in the alkaline state, likely due to the ionization of the functional group affecting the electron distribution and causing an increase in the maximum wavelength. For the AP-NPs spectrum (Figure 3B), at pH 2-10 the resulting absorbance intensity was lower than that of *A. paniculate*. The absorbance intensity at low pH was lowwer compared to neutral, and alkaline pH, but still more stable than *A. paniculata*. This indicates the presence of hypochromic shifts at low pH, and hyperchromic shift at neutral and alkaline pH but to a lesser extent. Despite these shifts, AP-NPs appear to maintain a more stable molecular structure compared to *A. paniculata*. It has been shown that nanoencapsulation is effective in stabilizing herbal extracts under various pH conditions (2-10).
The results of turbidity measurements (Figure 4) showed that at pH 2, *A. paniculata* had low turbidity, but the turbidity increased drastically at pH 3-4, with the highest turbidity of about 87 NTU obtained at pH 3. This indicates coagulation or deposition of active particles under acidic conditions. Above pH 4, the turbidity decreased, indicating particle deposition. It is known that active compounds can be damaged or degraded due to extreme conditions, such as acidic pH.[14]

Meanwhile, in the pH range of 2-10, AP-NPs showed low and stable turbidity, signaling that nanoencapsulation effectively prevented aggregation and maintained particle stability in a wide range of pH conditions, especially in acidic conditions that would normally cause instability.
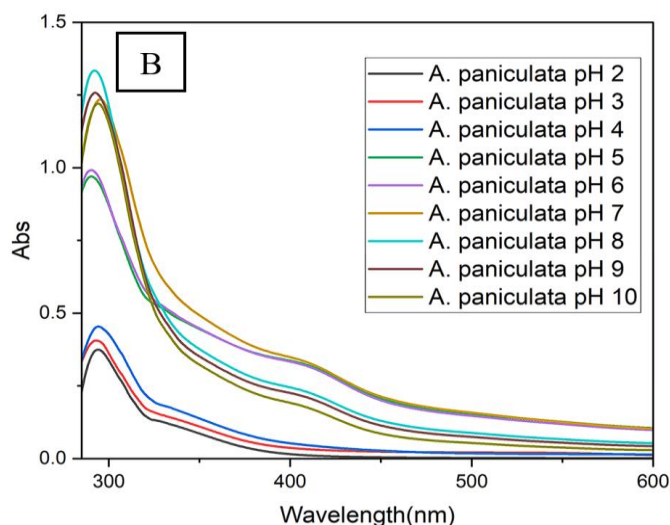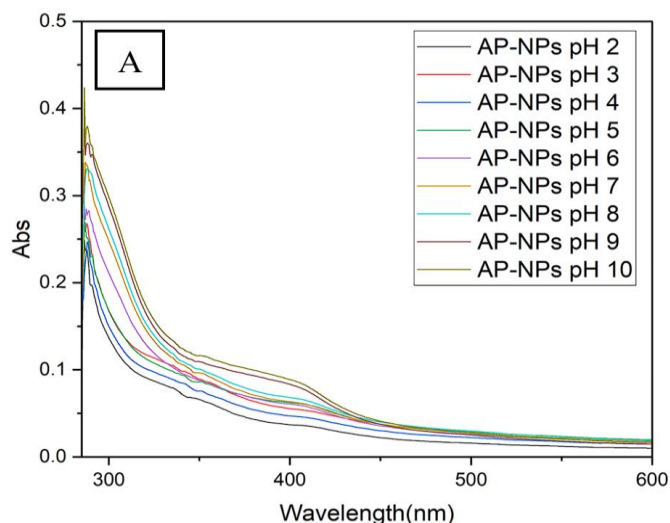
The stability of AP-NPs and *A. paniculata* was carried out at different temperatures, namely; by heating them at 30-100°C. The results showed that there is a difference in absorbance intensity caused by temperature changes (Figure 5). It was observed that the temperature change of 30-100°C drastically increased the absorbance of *A.*

Figure 3: Effect of pH on UV-Vis spectra of **(A)** AP-NPs, **(B)** A. paniculata

Paniculata, indicating the degradation of active compounds by temperature changes. Hypochromic shifts occur in both the spectrum of *A. paniculata* and AP-NPs, but in the presence of nanoencapsulation with CMC biopolymer as a coating of active compounds, AP-NPs showed higher stability at various temperature conditions characterized by the low absorbance intensity produced. Nanoencapsulation serves as a protective barrier that prevents active molecules from undergoing significant changes in their structure or reactivity to the environment, resulting in a more consistent spectrum with lower intensity, but stable over a wide range of temperatures.[31] Based on the turbidity graph on temperature variation (Figure 6), AP-NPs were more stable than *A. paniculata* on temperature changes. Nanoencapsulation successfully prevents coagulation or particle deposition that normally occurs at high temperatures, which is evident from the lower and consistent turbidity. In contrast, the turbidity of *A. paniculata* was high at low temperatures (about 21 NTU at 30°C) and decreased significantly as the temperature increased, reaching about 12 NTU at 60°C. Beyond this temperature, the turbidity was relatively stable up to 100°C. A decrease in turbidity at higher temperatures may indicate that the particles in *A. paniculata* undergo precipitation or coagulation as the temperature increases, leading to a decrease in the number of dispersed particles in the solution. This suggests that *A. paniculata* is more susceptible to clumping and precipitation at high temperatures which reduces its stability.
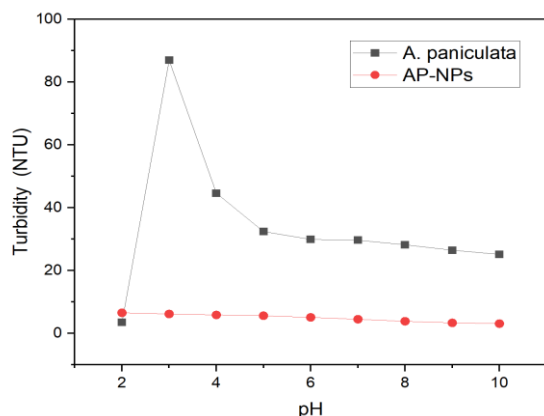
The stability of the nanocapsules was also assessed at varying electrolyte concentrations (0 – 0.3 M NaCl). It is known that the level of electrolytes in human blood is around 135-145 mmol/L.[32,33] The FTIR spectrum showed that the addition of NaCl to *A. paniculata* resulted in a bathochromic shift accompanied by a decrease in absorbance intensity, indicating a hypochromic shift (Figure 7). *A. paniculata* had a higher absorbance intensity compared to AP-NPs, indicating that the nanoencapsulation process was able to maintain the stability of the active compound under various concentrations of NaCl. The results of turbidity measurements (Figure 8) showed that the addition of NaCl at a concentration of 0.1 M caused an increase in turbidity up to 71 NTU, which may be due to decreased solubility and increased particle aggregation, a phenomenon known as salting out.[34] In addition, the salt ions neutralize the surface charge of *A. paniculata* particles, thereby reducing the repulsive force between the particles,[35] which ultimately leads to aggregation and increased turbidity. After reaching its peak (0.1 M), larger particles begin to settle, so the turbidity decreases, which is characterized by the formation of deposits or crusts at the bottom of the tube. In addition, AP-NPs exhibited lower and stable turbidity due to nanoencapsulation, which protects the active particles from the effects of aggregation caused by the addition Of NaCl. Nanoencapsulation creates particles that are more resistant to changes in the ionic environment, maintaining stability and a more uniform distribution of particles.

Table 2: Antidengue activity of *A. Paniculata* and AP-NPs

Sample	EC_{50} (μg/mL)	CC_{50} (μg/mL)	SI
A. Paniculata	9.87 ± 0.13	1522.95 ± 9.16	154.30
AP-NPs	68.12 ± 4.76	734.56 ± 11.72	10.78

Values are Mean ± Standard Error of Mean (SEM). EC_{50}: Effective concentration 50%, CC_{50}: Cytotoxic Concentration 50%, SI (Selectivity Index): The ratio between CC_{50} and EC_{50}.

Loading and release of A. paniculate nanocapsules
The loading of bioactive components in AP-NPs was determined through the percentage loading amount (% LA) and loading efficiency (% LE). The number of AP-NPs loaded was up to $27.18 \pm 2.51\%$, which reflects the total percentage of *A. paniculata* components that are successfully trapped in the nanocapsules. Meanwhile, the loading efficiency of AP-NPs was $54.36 \pm 5.02\%$, indicating the percentage of
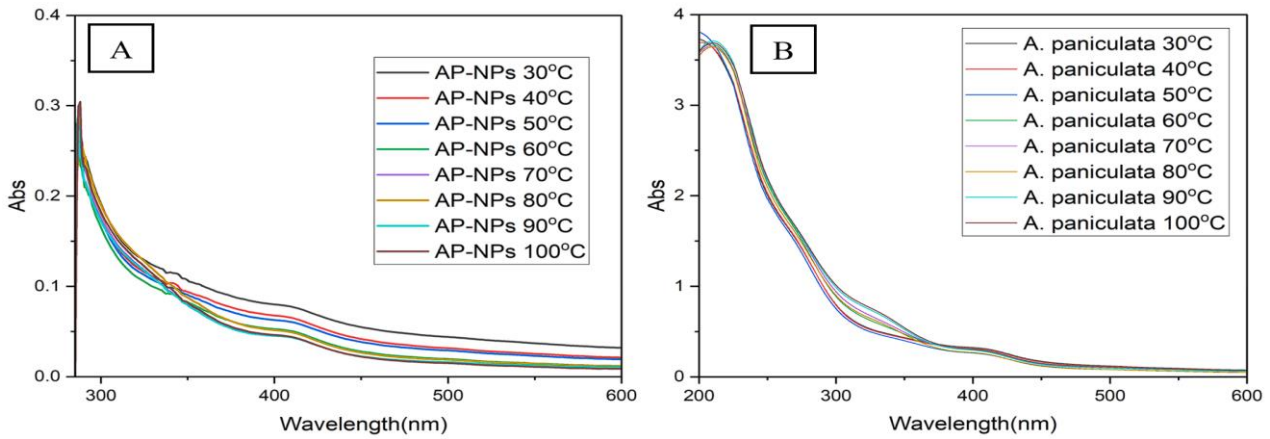

Figure 4: Effect of pH on turbidity of AP and AP-NPs

Figure 5: Effect of temperature on UV-Vis spectra of **(A)** AP-NPs, **(B)** *A. Paniculata*
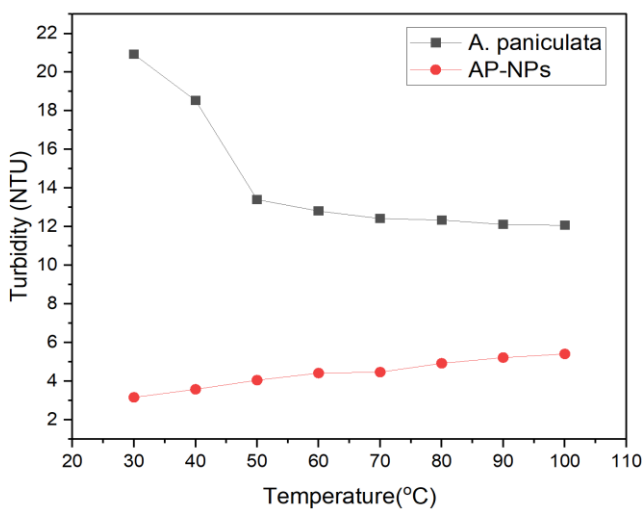

Figure 6: Effect of temperature on turbidity of AP and AP-NPs

A. paniculata components effectively incorporated in the nanocapsule micelles. The percentage release of bioactive components from AP-NPs was tested in a simulated human digestive system with pH variations of 2, 7, and 8.5 over 8 hours and the results were expressed in the form of a release percentage equivalent to quercetin. At pH 2, the discharge after 8 hours was only $52.46 \pm 2.58\%$, while at pH 7 the discharge increased to $61.14 \pm 8.71\%$, and the highest discharge ($74.94 \pm 6.33\%$) was at pH 8.5 (Figure 9). The low release at pH 2 is likely due to the aggregation of CMC polymers that occur under acidic conditions. It is known that CMCs begin to aggregate at pH <7 and this aggregation can inhibit the dissociation of the nanocapsules, thereby effectively blocking the release of bioactive components.[26]

Higher release of bioactive components was observed at neutral and alkaline pH (pH 7 and 8.5), suggesting that pH > 7 was the optimal condition for the release of bioactive components. At this pH, the solubility of CMC increases significantly, allowing the polymer to dissociate more easily and release the encapsulated bioactive component in the nanocapsule.
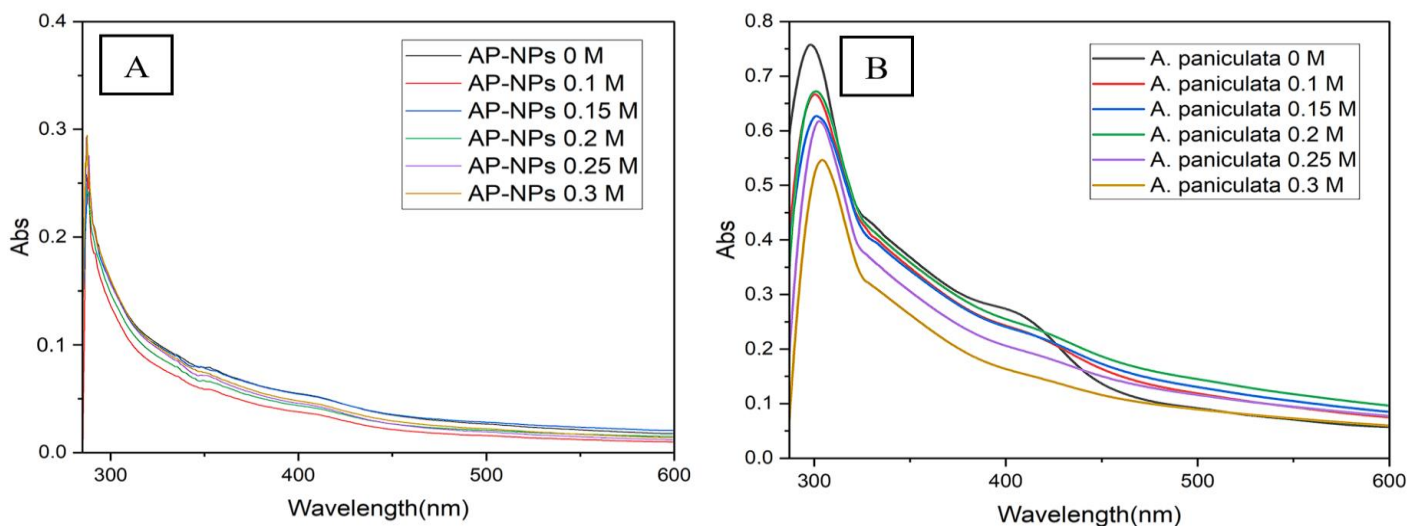

Figure 7: Effect of NaCl concentration on UV-Vis spectra of **(A)** AP-NPs, **(B)** *A. Paniculata*
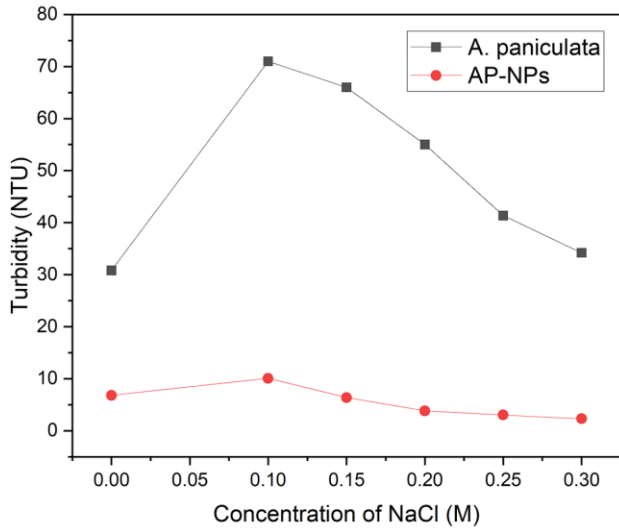
Figure 8: Effect of NaCl concentration on turbidity of AP and AP-NPs

In addition, at alkaline pH, the electrostatic interaction between the polymer and the bioactive component is reduced due to the change in charge. At high pH, the carboxyl group ($-COO^-$) in CMC undergoes deprotonation, making the polymer negatively charged. This condition reduces interaction with bioactive components that are also negatively charged, resulting

in a repulsive force. This repulsion reduces electrostatic interactions, promotes the release of bioactive components from the polymer rmatrix, and increases the overall release rate. As a result, a pH greater than 7 creates more favourable conditions for the release of bioactive components from AP-NPs.

Antidengue activity

The EC_{50} and CC_{50} values of *A. paniculata* extract and AP-NPs are shown in Table 2. The CC_{50} values of *A. paniculata* extract and AP-NPs were 1522.95 ± 9.16 μg/mL and 734.56 ± 11.72 μg/mL, respectively. This suggests that the toxicity of AP-NPs to cells is much higher than that of *A. paniculata* extract, as lower CC_{50} values indicate that lower concentrations of AP-NPs can already cause toxic effects (Figure 10B). Meanwhile, the EC_{50} value of *A. paniculata* extract was 9.87 ± 0.13 μg/mL, indicating that the extract has a strong potential in inhibiting dengue virus.
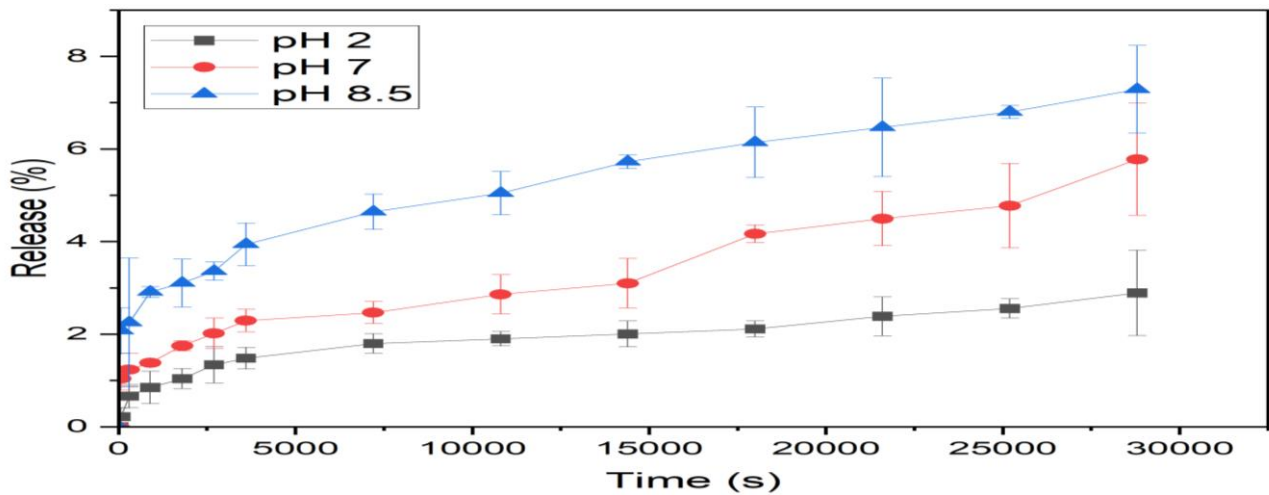

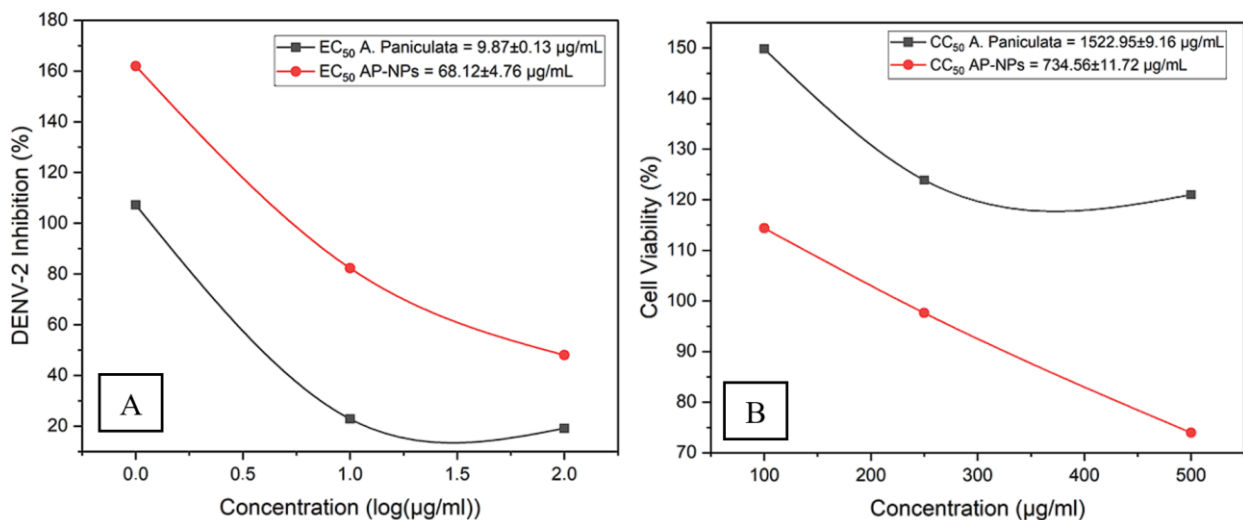**Figure 8:** The percentage release of quercetin in AP-NPs

Figure 9: The dose-response curves (**A**) the EC_{50} values, representing the effective concentration needed to achieve 50% of the desired biological activity, and (**B**) the CC_{50} values, indicating the concentration at which 50% of cells are rendered non-viable. These measurements compared *A. paniculata* extract and its nanocapsule (AP-NPs)

However, AP-NPs had a higher EC_{50} value, i.e. 68.12 ± 4.76 μg/mL, which means that a higher concentration of AP-NPs is required to achieve 50% viral inhibition compared to *A. paniculata* extract (Figure 10A). Nonetheless, AP-NPs still showed good antidengue potential, given that the encapsulation capabilities in AP-NPs can improve the bioavailability and stability of the active compounds in *A. paniculata*. This effectiveness could also be related to the gradual release of bioactive components from the nanocapsules, which can provide a longer-lasting anti-viral effect. *A. paniculata* extract showed an SI of 154.30, indicating a high level of safety and selectivity. In contrast, AP-NPs had an SI of 10.78, which was close to the previously reported SI value of 11.8,[12] indicating lower selectivity compared to pure extract but still promising as a therapeutic candidate. The findings from this study demonstrates the potential of CMC-based *A. paniculata* nanoencapsulation as an antidengue therapeutic candidate with better controlled release and enhanced bioactivity of the encapsulated active components.

Conclusion

This study successfully synthesized and characterized carboxymethyl chitosan-based *A. paniculata* nanocapsules for antiviral therapy against dengue. Nanoencapsulation enhanced the stability, bioavailability, and controlled release of bioactive compounds from *A. paniculata*, allowing for more effective antiviral action. While the nanoencapsulated formulation (AP-NPs) demonstrated improved stability and gradual release, the toxicity levels were higher than the non-encapsulated extract. Nevertheless, these nanoformulations show significant potential in dengue treatment due to their prolonged antiviral effect and enhanced bioactivity. Further research is recommended to optimize the formulation and reduce toxicity for clinical applications

Conflict of Interest

All the authors declare no conflicts of interest.

Authors' Declaration

The authors hereby declare that the work presented in this article is original and that any liability for claims relating to the content of this article will be borne by them.

Acknowledgements

References

1. European Centre for Disease Prevention and Control. Dengue Worldwide Overview. [Internet]. Available from: https://ecdc.europa.eu/en/dengue-monthly [Accessed Dec 12, 2024].
2. Zerfu B, Kassa T, Legesse M. Epidemiology, biology, pathogenesis, clinical manifestations, and diagnosis of dengue virus infection, and its trend in Ethiopia: A comprehensive literature review. Trop Med Health. 2023; 51(1):11. https://doi.org/10.1186/s41182-023-00504-0.
3. Amorim MT, Hernández LH, Naveca FG, Essashika Prazeres IT, Wanzeller ALM, Silva EVPD, Casseb LMN, Silva FSD, da Silva SP, Nunes BTD, Cruz ACR. Emergence of a new strain of DENV-2 in South America: Introduction of the cosmopolitan genotype through the Brazilian-Peruvian border. Trop Med Infect Dis. 2023;8(6):325. https://doi.org/10.3390/tropicalmed8060325.
4. Kok BH, Lim HT, Lim CP, Lai NS, Leow CY, Leow CH. Dengue virus infection—a review of pathogenesis, vaccines, diagnosis, and therapy. Virus Res. 2023; 324:199018. https://doi.org/10.1016/j.virusres.2022.199018.
5. Pajor MJ, Long B, Liang SY. Dengue: A focused review for the emergency clinician. Am J Emerg Med. 2024; 82:82–87. https://doi.org/10.1016/j.ajem.2024.05.022.
6. Wardana AP, Aminah NS, Kristanti AN, Fahmi MZ, Abdjan MI, Teguh H. Species used as herbal medicine in Indonesia. Trop J Nat Prod Res. 2024; 8(9):8393–8399. https://doi.org/10.26538/tjnpr/v8i9.22.
7. Rafi M, Karomah AH, Heryanto R, Septaningsih DA, Kusuma WA, Amran MB, Rohman A, Prajogo B. Metabolite profiling of *Andrographis paniculata* leaves and stem extract using UHPLC-Orbitrap-MS/MS. Nat Prod Res. 2022; 36(2):625–629. https://doi.org/10.1080/14786419.2020.1789637.
8. Irawan C, Enriyani R, Ismail, Sukiman M, Putri ID, Utami A, Rahmatia L, Lisandi A. Effects of solvent variation on the antioxidant, anti-inflammatory, and alpha-glucosidase inhibitory activity of *Andrographis paniculata* leaves extract. Trop J Nat Prod Res. 2024; 8(1):5968–5972. https://doi.org/10.26538/tjnpr/v8i1.36.
9. Ramalingam S, Karupannan S, Padmanaban P, Vijayan S, Sheriff K, Palani G, Krishnasamy KK. Anti-dengue activity of *Andrographis paniculata* extracts and quantification of dengue viral inhibition by SYBR Green reverse transcription polymerase chain reaction. Ayu. 2018; 39(2):87–91. https://doi.org/10.4103/ayu.AYU_144_17.
10. Nguyen HT, Do VM, Phan TT, Nguyen Huynh DT. The potential of ameliorating COVID-19 and sequelae from *Andrographis paniculata* via bioinformatics. Bioinform Biol Insights. 2023;17: 11779322221149622. https://doi.org/10.1177/11779322221149622.
11. Intharuksa A, Arunotayanun W, Yooin W, Sirisa-ard P. A comprehensive review of *Andrographis paniculata* and its constituents as potential lead compounds for COVID-19 drug discovery. Molecules. 2022; 27(14): 4479. https://doi.org/10.3390/molecules27144479.
12. Dewi BE, Desti H, Ratningpoeti E, Sudiro M, Fithriyah, Angelina M. Effectivity of quercetin as antiviral to dengue virus-2 strain New Guinea C in Huh 7-It 1 cell line. IOP Conf Ser Earth Environ Sci. 2020; 462(1):012033. https://doi.org/10.1088/1755-1315/462/1/012033.
13. Sun D, Gao W, Hu H, Zhou S. Why 90% of clinical drug development fails and how to improve it? Acta Pharm Sin B. 2022; 12(7):3049–3062. https://doi.org/10.1016/j.apsb.2022.02.002.
14. Hua S. Advances in oral drug delivery for regional targeting in the gastrointestinal tract—influence of physiological, pathophysiological, and pharmaceutical factors. Front Pharmacol. 2020; 11:1–22. https://doi.org/10.3389/fphar.2020.00524.
15. Delshadi R, Bahrami A, McClements DJ, Moore MD, Williams L. Development of nanoparticle-delivery systems for antiviral agents: A review. J Control Release. 2021; 331:30–44. https://doi.org/10.1016/j.jconrel.2021.01.017.
16. Cahyaningrum SE, Amaria, Muhaimin FI. The kinetic release and in-vivo study of alginate-chitosan encapsulated metformin against type II diabetes mellitus. Rasayan J Chem. 2022;15(2):1040–1044. https://doi.org/10.31788/RJC.2022.1526763.
17. Ravi H, Kurrey N, Manabe Y, Sugawara T, Baskaran V. Polymeric chitosan-glycolipid nanocarriers for an effective delivery of marine carotenoid fucoxanthin for induction of apoptosis in human colon cancer cells (Caco-2 cells). Mater Sci Eng C Mater Biol Appl. 2018; 91:785–797. https://doi.org/10.1016/j.msec.2018.06.018.

18. Costa JR, Xavier M, Amado IR, Gonçalves C, Castro PM, Tonon RV, Cabral LMC, Pastrana L, Pintado ME. Polymeric nanoparticles as oral delivery systems for a grape pomace extract towards the improvement of biological activities. Mater Sci Eng C. 2021; 119:111551. https://doi.org/10.1016/j.msec.2020.111551.

19. Jafernik K, Ładniak A, Blicharska E, Czarnek K, Ekiert H, Wiącek AE, Szopa A. Chitosan-based nanoparticles as effective drug delivery systems—a review. Molecules. 2023; 28(4):1963. https://doi.org/10.3390/molecules28041963.

20. Suryani S, Chaerunisaa AY, Joni IM, Ruslin R, Aspadiah V, Anton A, Sartinah A, Ramadhan OAN. The chemical modification to improve solubility of chitosan and its derivatives: application, preparation method, toxicity as a nanoparticle. Nanotechnol Sci Appl. 2024;17:41–57. https://doi.org/10.2147/NSA.S450026.

21. Azman M, Sabri AH, Anjani QK, Mustaffa MF, Hamid KA. Intestinal absorption study: challenges and absorption enhancement strategies in improving oral drug delivery. Pharmaceuticals. 2022;15(8):975. https://doi.org/10.3390/ph15080975.

22. Tobias A and Sadiq NM. Physiology, gastrointestinal nervous control; In StatPearls [Internet]. StatPearls Publishing: Treasure Island (FL); 2024. PMID: 31424852..

23. Liu Y, Sun M, Wang T, Chen X, Wang H. Chitosan-based self-assembled nanomaterials: their application in drug delivery. View. 2021; 2(1):1-13. https://doi.org/10.1002/VIW.20200069.

24. Noore S, Rastogi NK, O'Donnell C, Tiwari B. Novel bioactive extraction and nano-encapsulation. Encyclopedia. 2021; 1(3):632–664. https://doi.org/10.3390/encyclopedia1030052

25. Wardana AP, Aminah NS, Novi A, Kristanti A, Manuhara YSW, Fahmi MZ, Sucipto TH, Abdjan MI, Indriani. *Gynura procumbens* nanoencapsulation: A novel promising approach to combat dengue infection. Rasayan J Chem. 2023;16(2):0976–0983. https://doi.org/10.31788/rjc.2023.1628298.

26. Kalliola S, Repo E, Srivastava V, Zhao F, Heiskanen JP, Sirviö JA, Liimatainen H, Sillanpää M. Carboxymethyl chitosan and its hydrophobically modified derivative as pH-switchable emulsifiers. Langmuir. 2018;34(8):2800–2806. https://doi.org/10.1021/acs.langmuir.7b03959.

27. Sucipto TH, Setyawati H, Churrotin S, Amarullah IH, Sumarsih S, Wardhani P, Aryati A, Soegijanto S. Anti-dengue type 2 virus activities of zinc (II) complex compounds with 2-(2,4-dihydroxyphenyl)-3,5,7-trihydroxycromen-4-one ligands in Vero cells. Indones J Trop Infect Dis. 2019;7(5):105. https://doi.org/10.20473/ijtid.v7i5.10851.

28. Khan I, Saeed K, Khan I. Nanoparticles: properties, applications, and toxicities. Arab J Chem. 2019; 12(7):908–931. https://doi.org/10.1016/j.arabjc.2017.05.011.

29. Danaei M, Dehghankhold M, Ataei S, Hasanzadeh Davarani F, Javanmard R, Dokhani A, Khorasani S, Mozafari MR. Impact of particle size and polydispersity index on the clinical applications of lipidic nanocarrier systems. Pharmaceutics. 2018; 10(2):87. https://doi.org/10.3390/pharmaceutics10020057.

30. Koshani R and Jafari SM. Ultrasound-assisted preparation of different nanocarriers loaded with food bioactive ingredients. Adv Colloid Interface Sci. 2019; 270:123–146. https://doi.org/10.1016/j.cis.2019.06.005.

31. Pateiro M, Gómez B, Munekata PES, Barba FJ, Putnik P, Kovačević DB, Lorenzo JM. Nanoencapsulation of promising bioactive compounds to improve their absorption, stability, functionality, and the appearance of the final food products. Molecules. 2021; 26(6):1547. https://doi.org/10.3390/molecules26061547.

32. Ambati R, Kho LK, Prentice D, Thompson A. Osmotic demyelination syndrome: novel risk factors and proposed pathophysiology. Intern Med J. 2023; 53(7):1154–1162. https://doi.org/10.1111/imj.15855.

33. Buffington MA and Abreo K. Hyponatremia: a review. J Intensive Care Med. 2016; 31(4):223–236. https://doi.org/10.1177/0885066614566794.

34. Nishida K, Morita H, Katayama Y, Inoue R, Kanaya T, Sadakane K, Seto H. Salting-out and salting-in effects of amphiphilic salt on cloud point of aqueous methylcellulose. Process Biochem. 2017; 59:52–57. https://doi.org/10.1016/j.procbio.2016.12.009.

35. Nugraheni PS, Soeriyadi AH, Sediawan WB, Ustadi, Budhijanto W. Influence of salt addition and freezing-thawing on particle size and zeta potential of nano-chitosan. IOP Conf Ser Earth Environ Sci. 2019; 278(1):012052. https://doi.org/10.1088/1755-1315/278/1/012052.